HHS Public Access

Author manuscript

Cortex. Author manuscript; available in PMC 2019 November 01.

Published in final edited form as:

Cortex. 2018 November ; 108: 252–264. doi:10.1016/j.cortex.2018.08.002.

Altered topology of the functional speech production network in non-fluent/agrammatic variant of PPA

ML Mandelli[1], **E Vilaplana**[2,3], **AE Welch**[1], **C Watson**[1], **G Battistella**[1], **JA Brown**[1], **KL Possin**[1], **HI Hubbard**[4], **ZA Miller**[1], **ML Henry**[5], **GA Marx**[1], **MA Santos-Santos**[6,7], **LP Bajorek**[1], **J Fortea**[2], **A Boxer**[1], **G Rabinovici**[1], **S Lee**[1], **J Deleon**[1], **HJ Rosen**[1], **BL Miller**[1], **WW Seeley**[1,8], and **ML Gorno-Tempini**[1]

[1]Department of Neurology, Memory and Aging Center, University of California San Francisco, CA, USA

[2]Memory Unit, Department of Neurology, Hospital de la Santa Creu i Sant Pau - Biomedical Research Institute Sant Pau – Universitat Autonoma de Barcelona, Spain

[3]Centro de Investigacion Biomedica en Red de Enfermedades Neurodegenerativas – CIBERNED, Spain

[4]Department of Communication Science and Disorders, Faculty of Rehabilitation Medicine, University of Alberta, Edmonton, AB, Canada

[5]Department of Communication Sciences and Disorders, University of Texas, Austin USA

[6]Cognition and brain plasticity group [Bellvitge biomedical research institute-IDIBELL], L'Hospitalet de Llobregat, Barcelona, Spain

[7]Fundació ACE memory clinic and research center, Institut Catalá de neurociències aplicades, Barcelona, Spain

[8]Department of Pathology, University of California San Francisco, CA, USA

Keywords

primary progressive aphasia; functional connectivity; graph theory; speech production network; topological configuration

1. Introduction

The non-fluent/agrammatic variant of primary progressive aphasia (nfvPPA) is a neurological syndrome that falls under the umbrella of frontotemporal dementia (FTD) (Mesulam 1982). In particular, this variant is characterized by isolated and progressive

Correspondence to: Maria Luisa Mandelli, 675 Nelson Rising Lane, Mission Bay Campus, San Francisco, CA 94158, MariaLuisa.Mandelli@ucsf.edu.

motor speech and/or grammatical impairments with anatomical damage in regions associated with speech production functions (Gorno-Tempini et al., 2004; Grossman 2012). Several neuroimaging studies of nfvPPA have shown gray matter atrophy and hypometabolism in left fronto-insular cortical and subcortical regions, particularly the inferior frontal gyrus (IFG), precentral gyrus, supplementary motor cortex (SMC), anterior dorsal insula, and striatum (Grossman et al., 1996; Nestor et al., 2003; Gorno-Tempini et al., 2006). Other studies have described structural damage to dorsal white matter pathways connecting these regions and associated speech and language deficits (Galantucci et al., 2011; Wilson et al., 2011; Catani et al., 2013; Mandelli et al., 2014). More recent researches suggest that functional changes precede structural alterations (Taubert et al., 2011, Bonakdarpour et al., 2017).

Resting state functional MRI (rsfMRI) studies have shown how distant brain regions interact with each other to form large-scale intrinsic connectivity networks (ICNs) (Biswal et al., 1995; Greicius et al., 2003; Damoiseaux et al., 2006). Recent studies demonstrated that anatomical damage caused by various neurodegenerative disorders targets specific ICNs identified in healthy subjects (Zhou et al., 2012; Mandelli et al., 2016; Collins et al., 2017). This supports a network degeneration hypothesis in which neurodegeneration begins in particular regions and spreads along disease-specific pathways to other regions within and outside the network as the disease progresses (Frost & Diamond, 2010; de Calignon et al., 2012; Liu et al., 2012).

In nfvPPA, we have previously hypothesized that focal atrophy occurs first in the left inferior frontal gyrus and then progresses to areas most structurally and functionally connected within a network that has been described as the *speech production network* (SPN) (Mandelli et al., 2016).

Within the various analytical approaches to investigate network connectivity, graph theoretical methods model the brain as a complex network and provide metrics that reflect global or local organization, such as global efficiency, characteristic path length, modularity, and clustering coefficient (Strogatz 2001; Sporns et al., 2004; Watts 2004; Boccaletti et al., 2006; Bullmore & Sporns, 2009; Stam & Reijneveld, 2007, Minati et al., 2013, Tijms et al, 2013). Multicenter and longitudinal studies comparing different connectivity methods showed that graph theory provides reliable, replicable and robust measures of network abnormalities in patients with frontotemporal dementia (FTD) (Sedeño et al., 2017) as well as the best unit-wise reliability (Guo et al., 2012). This evidence suggests that graph theory is uniquely suited to studying network dynamics in focal neurodegenerative diseases (Horwitz & Rowe, 2011).

Several studies have attempted to investigate alterations of functional network connectivity and network topology in neurodegenerative disorders such as Alzheimer's disease or FTD using rsfMRI and graph theory (Stam et al., 2007; Supekar et al., 2008; Sanz-Arigita et al., 2010; Zhao et al., 2012; Agosta et al., 2013; Agosta et al., 2014; Sedeño et al., 2016). However, no published studies have assessed network properties in nfvPPA using graph theory.

In this study, we applied graph theoretical analysis to describe alterations within the organization of the SPN in nfvPPA. NfvPPA provides a good model to study network alterations because the anatomical damage is initially confined to a network that is anatomically and functionally welldescribed. We investigated functional specialization (segregation), information flow (integration), resilience (assortativity), and centrality (hubness) within the SPN and a reference network, the default mode network (DMN). We hypothesized the topological architecture of the SPN and not the DMN would be preferentially disrupted in nfvPPA due to the focal damage in the left fronto-insular regions.

2. Material and Methods

2.1 Subjects

We identified 20 patients with a diagnosis of nfvPPA seen at the Memory and Aging Center (MAC) of the University of California, San Francisco (UCSF). These twenty patients underwent a comprehensive research evaluation, including a neurological examination with a behavioral neurologist, neuropsychological testing, speech and language testing with a speech pathologist, and a high-resolution structural T1-weighted and rsfMRI. The attending behavioral neurologist determined a diagnosis based on behavioral performance, patient and family history, neuroimaging, and a second neurological examination. The patients were diagnosed in accordance with the international consensus criteria for the nfvPPA developed by Gorno-Tempini et al. (2011). The criteria include one of the following: 1) agrammatism in language production (oral or written); 2) effortful, halting speech with inconsistent speech sound errors and distortions (apraxia of speech), and at least two of the following criteria: 1) impaired comprehension of syntactically complex sentences; 2) spared single-word knowledge; 3) spared object knowledge.

A group of 20 healthy controls without cognitive or neurological deficits were selected from the MAC database and matched to the patient group according to age, gender, handedness, and education.

Informed consent was obtained from all participants in accordance with the Declaration of Helsinki and approval was obtained from the UCSF Committee on Human Research.

2.2 General Cognitive Evaluation

Patients underwent neuropsychological assessment as previously described in Kramer et al., 2003, Rosen et al., 2002 and Gorno-Tempini et al., 2004. Global cognitive functioning was assessed with the mini-mental state examination (MMSE) (Folstein et al., 1975). Visuospatial skills were assessed by the Benson figure copy, and memory was assessed by the California Verbal Learning Test – Short Form (CVLT-SF) as well as a 10-minute free recall of the Benson complex figure. Executive function, including attention, working memory, and processing speed were assessed via forward and backward digit span, phonemic fluency (D words generated in 1 minute), and a modified version of the Trails B test.

2.3 Speech and Language Evaluation

NfvPPA patients completed a linguistic evaluation with a speech-language pathologist (Gorno-Tempini et al., 2004; Wilson et al., 2010). A motor speech evaluation (Wertz et al. 1984) described the presence of apraxia of speech and/or dysarthria. Syntax comprehension was tested using a two-alternative forced choice auditory sentence-to-picture matching task (Wilson et al., 2010). We tested naming via the 15-item Boston Naming Test (Kramer et al., 2003). Subtests from the Western Aphasia Battery (WAB) (Kertesz, 1980) included Spontaneous Speech (Information content and Fluency), Auditory Word Recognition, Sequential Commands, and Repetition. Semantics were evaluated using the Pyramids and Palm Trees Picture Test (Howard & Patterson, 1992).

2.4 MRI Sequences

All subjects underwent an MRI on a 3T Siemens scanner TrioTim syngo, equipped with an eight-channel transmit-and-receive head coil, using a magnetization prepared rapid gradient echo (MPRAGE) sequence (160 sagittal slices; slice thickness = 1 mm; field of view = 256 mm^2; matrix = 256 × 240; voxel size 1.0 × 1.0 × 1.0 mm^3; repetition time = 2300 ms; echo time = 2.98 ms; inversion time = 900 ms; flip angle = 9°). RsfMRI data used a T2*-weighted echo-planar sequence including 240 volumes with 36 AC/PC-aligned axial slices in interleaved order (slice thickness = 3 mm with 0.6 mm gap; field of view = 230 × 230 mm; matrix = 92 × 92; TR = 2000 ms; TE = 27 ms; flip angle = 80°). During task-free resting state sequences, the subjects were asked to lie still and close their eyes without falling asleep.

2.5 Data Analysis

2.5.1 Structural imaging analysis—Voxel-based morphometry (VBM) analysis of the structural images was conducted using Statistical Parametric Mapping (SPM12) (Wellcome Trust Center for Neuroimaging, London, UK; http://www.fil.ion.ucl.ac.uk/spm/software/spm12/) running on Matlab R2013a (MathWorks). The preprocessing has been previously described (see Mandelli et al., 2016 for more details). Structural images were segmented into gray matter (GM), white matter, (WM) and cerebrospinal fluid (CSF) using an adaptive maximum a posteriori technique (Rajapakse et al., 1997), which were then registered to a standard space (MNI) and modulated by the Jacobian determinant to preserve the relative GM volume. Images were smoothed for statistical analysis (8 mm full-width at half-maximum [FWHM] Gaussian kernel mm). A general linear model of the GM maps was performed using age, sex, and total intracranial volume (TIV) as covariates to confirm the pattern of gray matter atrophy in this group of patients.

2.5.2 Resting state functional MRI analysis—Pre-processing of the functional images was performed as previously described (Mandelli et al., 2016). After discarding the first eight volumes of each run, functional data sets were slice-time corrected, spatially realigned, skull-stripped, co-registered to the structural T1-weighted image, normalized, and smoothed with a 6 mm full-width at half-maximum Gaussian kernel. Normalization was achieved by calculating the transformation parameters between the subject's T1 anatomical image and the MNI T1-weighted image template and applying those parameters to the

functional dataset. The functional datasets were band-pass filtered (0.008 Hz < f < 0.15 Hz), and the nuisance variables were regressed out from the data, which included six motion parameters, CSF, and WM time-series as well as the first derivative and quadratic terms (Satterthwaite et al., 2013).

Intrinsic connectivity networks (ICNs) defined by seed ROIs in healthy controls: Intrinsic connectivity networks (ICNs) of interest were extracted by using a seed-based ROI approach in 20 patients and 20 matched control subjects. The seed ROI of the SPN was a sphere of 4 mm radius located in the pars opercularis of the left inferior frontal gyrus (MNI: × = -48, y = 15, z = 23), an area identified by a previous VBM study of a group of mild nvfPPA patients (Clinical Dementia Rating CDR=0) as the earliest locus of atrophy (Mandelli et al., 2016). The patient group from this 2016 article was independent from the patient group in this study. The DMN seed ROI was a sphere of 4 mm radius centered in the precuneus (MNI: × = 2, y = -51, z = 27) (Greicius et al., 2004; Damoiseaux et al., 2006). The DMN was considered a reference network for this analysis.

For each subject, seed ROIs were reverse-normalized to the subject's fMRI native space. Then, the average time-series was extracted from the fully processed rsfMRI images and used to compute the temporal correlation against all other voxels in the brain to create an r-Pearson correlation map of each voxel's connectivity strength to the seed ROI. The r-Pearson correlation maps were transformed into Z-scores using Fisher's r to Z transformation and then normalized to MNI space.

The ICNs were obtained at group level for both controls and patients by performing one-sample t-tests of the Z score maps in SPM12. Age, gender, and TIV were used as covariates. The statistical threshold was set at P < 0.001, corrected for family wise error (FWE). The resulting two ICN maps (one each for the SPN and DMN) were used as masks to define the areas of interest for the following analysis.

2.5.3 Graph theory analysis—Graph theory analysis has recently been applied to neuroscientific research to describe and quantify the topology of brain network architecture. In graph theory, a network is modeled as a graph that is defined by nodes and edges and mathematically represented by adjacency matrices. Nodes are defined as cortical regions or signal recording sites, and edges represent the connectivity between nodes, extracted from a structural or functional dataset (Rubinov & Sporns 2010). In this study, we aim to represent the architecture of the SPN using graph theory based on functional connectivity data. This network is of particular interest because it is anatomically and functionally well-described and selectively affected in nfvPPA patients. The procedure for graph theoretical analysis of the functional connectivity data is described below.

2.5.3 A Graph construction: definition of nodes and edges.: Nodes were defined by subdividing cortical and subcortical regions of the healthy controls' ICN maps into non-overlapping cubes with 7 mm sides that were separated from each other by 1 mm. Edges were defined for each subject from the functional connectivity data represented by the Z score of r-Pearson correlation maps between each pair of nodes. The graphs are represented as adjacency matrices whose dimensions are equal to the total number of nodes. Each

position in the matrix corresponds to the strength of the functional connectivity between a pair of nodes. In order to create adjacency matrices, a thresholding method was employed. Different methods have been proposed in the literature: one option was to choose a relative threshold that identifies a certain percentage of the total number of connections for each subject (Tian et al., 2011; de Haan et al., 2009). This would produce the same number of connections for each subject, whether a patient or control. However, relative thresholds may obscure the differences in functional connectivity between patients and controls caused by disease (van Wijk et al, 2010; van den Heuvel et al., 2017). Therefore, to take into account this difference, we used an absolute threshold, as done in previous studies (Salvador et al., 2005; Meunier et al., 2009; van den Heuvel et al., 2010; Agosta et al., 2013; Agosta et al., 2014). To avoid bias toward a specific threshold, we selected a range of thresholds able to create a non-fragmented network with a minimum number of connections.

Once the brain graph was determined, its properties were quantified by using several topological measures at nodal or global level (Rubinov & Sporns 2010) over the entire range of chosen thresholds.

2.5.3.B Nodal measures: definition of hubs.: Some nodes in the graph have a particularly important role in the structural integrity or functional performance of the network. These nodes are called *hubs*. A hub's location in a network is critical for the efficiency of communications between nodes, and may facilitate connections between distant brain regions or, more locally, within a cluster that shares the same function (van de Heuvel & Sporns 2013). There is no single way to define the hubs in a network. Rather, multiple different measures, called *measures of influence,* are employed (Sporns et al., 2007). The most common measure to define the hubs is called the *nodal degree,* calculated as the number of edges that are connected to that node. This measure is an index of connectivity of a node with the rest of the nodes in a network. Another measure used to define hubs is *betweenness centrality,* which calculates the fraction of all shortest paths in the network that pass through a given node. This measure is an index of how centrally important a particular node is in the network pathways (Freeman 1977). In this study, nodal degree and betweenness centrality were calculated for each node and then integrated with the chosen range of thresholds for the statistical analysis. A node was therefore defined as hub when any of the two nodal parameters were at least one standard deviation higher than the average of the corresponding measure (degree or centrality) over the entire network for either patients or controls (Tian et al., 2011).

2.5.3.C Global measures.: Several metrics are available to describe the global properties of the network. They can be divided into two main categories: measures of integration and segregation. These measures describe how linked nodes allow information to flow from one region to another and how they organize themselves in communities for specialized functions. Measures of integration are based on path and indicate how efficiently brain regions can communicate with each other. For example, the shorter the path connecting two nodes, the faster and more efficient the flow of information between those nodes will be. The average of the shortest path length between all pairs of nodes is called the *characteristic path length* of the network while the inverse average of the shortest path is known as *global*

efficiency and represents the measure of overall information transfer efficiency across the network. Conversely, measures of segregation are based on communities or modules (groups of nodes that are more densely connected to each other than to other communities). These metrics indicate how the network is organized into subnetworks specialized in specific tasks while communicating with the rest of the network. The two most common measures of functional segregation are *modularity* and *cluster coefficient*. Modularity is calculated by dividing the network into groups of nodes that are maximally intraconnected and minimally interconnected with the other modules (Newman 2006; Blondel et al., 2008) by using algorithms of optimization. High modularity implies multiple segregated communities of nodes within the network. Cluster coefficient is calculated as the average fraction in which pairs of neighboring nodes are also neighbors of each other. Essentially, it is a normalized measure of loops with a path length of three, or nodes that form triangles (triangular connectivity relationships). It quantifies cliquishness and is related to local network efficiency (Latora & Marchori, 2001). While modularity looks at edge densities in given clusters compared to edge densities between clusters, cluster coefficient measures the density of triangles. Another interesting global metric is assortativity. In an assortative network, high-degree nodes (nodes that have the highest number of connections in the network) tend to connect to other high-degree nodes. In a dissortative network, they are more likely to be connected to low degree nodes. Assortativity is a measure of robustness and resilience: the removal of one high-degree node can be overcome by the interconnectedness of the others (Newman, 2002; Newman 2003).

Global metrics can be influenced by the network's density (the proportion of all possible connections present in the network), particularly when the absolute threshold is used (van Wijk et al., 2010). To correct for the possibility of different network densities between patients and controls, global metrics were normalized by dividing each metric by the mean across 20 random networks generated with the equivalent number of nodes, edges and degree distribution.

Graph analyses were conducted with GraphVar toolbox (Kruschwitz et al. 2015) on Matlab 2013a, which includes software packages such as Brain Connectivity Toolbox (Rubinov & Sporns 2010). BrainNet Viewer (http://www.nitrc.org/projects/bnv/) was used for network visualization (Xia et al., 2013).

2.5.3.D Statistical analysis of graph measures.: Global and nodal network parameters were compared between the two groups for each threshold with independent t-tests. Global results were corrected for multiple comparisons according to the number of connectivity metrics tested. The threshold for significance was set at $P = 0.01$. Nodal metric differences were investigated after computing the integrated global network parameters as the summation over the range of thresholds chosen. Nodal metrics were also adjusted for GM volume at each node as a confound in the analysis. Volume intensities were extracted from the normalized structural T1 images. Nodal metric results were also corrected for multiple comparisons (False Discovery Rate or FDR).

3. Results

3.1 Demographic and Clinical Data of nfvPPA

Demographic and clinical data of the subjects in the study are reported in Table 1. A pattern of speech and language deficits typical of nfvPPA was seen and all patients met nfvPPA criteria according to that set out in Gorno-Tempini 2011. Patients in this study had difficulty with syntax in a task designed to test comprehension of a range of syntactical structures, such as passive and active sentences. Patients also demonstrated motor speech patterns consistent with apraxia of speech and/or dysarthria, according to a speech pathologist performing a motor speech evaluation. Single word comprehension and object knowledge were spared, as tested in the Pyramids and Palm Trees Picture Test and oral picture descriptions. This group of patients was in the milder range of symptom progression, with a CDR of 0–1. Nevertheless, nineteen of the twenty patients had motor speech difficulties, mostly with mild to moderate apraxia of speech. All of the patients displayed simplified syntax in syntax production tasks or impaired comprehension of complex syntactical structures.

The pattern of atrophy was present in the left IFG, SMC, supramarginal gyrus, insula, and striatum and also in the right IFG, at a threshold of $P < 0.05$ corrected for FWE, in nfvPPA compared to controls in line with previous studies (Supplementary Figure 1). These are the regions of the SPN known to be atrophic in nfvPPA (Grossman et al., 1996; Nestor et al., 2003; Gorno-Tempini et al., 2006).

3.2 Intrinsic Connectivity Networks in healthy controls

ICN maps of the SPN and DMN were obtained from the group of healthy subjects and patients. As in our previous paper (Mandelli et al., 2016), the SPN involved brain regions of the left hemisphere including the IFG (opercularis and triangularis), the middle and superior frontal gyri, the precentral cortex, the SMC, the inferior parietal regions (supramarginal and angular gyri), superior parietal areas, the middle/inferior temporal gyrus, the anterior dorsal insula, and the striatum. Regions in the right hemisphere were also involved: IFG, SMC, inferior parietal lobe, caudate and the inferior temporal gyrus (Figure 1). According to the literature and our previous publication, the DMN involves the medial prefrontal and orbital cortices, the posterior cingulate cortex, the angular gyrus, and the medial temporal lobe (Greicius et al., 2004; Damoiseaux et al., 2006).

3.3 Graph Theory Analysis and Network Parameters

The spatial parcellation of the SPN resulted in 110 cortical and sub-cortical non-overlapping nodes, while the parcellation of the DMN produced 146 nodes. Adjacency matrices were obtained from the Z score maps of functional connectivity for each pair of nodes within the network and for each subject in both groups. For the patient group, the chosen thresholds varied over a range from 40% to 70% of connections in order to make the SPN and DMN comparable. This resulted in a range of thresholds from 0.1 to 0.3 for the SPN and from 0.2 to 0.4 for the DMN.

3.3.1 Hub organization within the speech production network.—SPN hubs in healthy controls were mainly left lateralized, and localized in the posterior and superior portion of the IFG opercularis, the precentral gyrus, the inferior and superior parietal lobe, the SMC, and posterior temporal regions (Supplementary Figure 2A). SPN hubs in nfvPPA were distributed more anteriorly in the left IFG and MFG and in the right IFG and MFG with greater loss of hubs in the parietal regions and SMC (Supplementary Figure 2B). Differences in the distribution of hubs in nfvPPA compared to controls are shown in Figure 2. For each of these hubs that were lost or new in nfvPPA, we calculated the Z score of GM volume and nodal metrics in the patient group. We then performed a two-sample t-test (one for each metric) between the average Z-scored metric in the lost hubs vs. the new ones. This analysis has been performed to understand if the different distribution of hubs was driven by the loss of volume. We found a significant decrease of the nodal degree in the lost hubs ($P<0.000$, Effect size = 1.6) and an increase of betweenness centrality ($P<0.000$, Effect size = 3.4) in the new hubs. No difference was observed in GM volume ($P=0.5$, Effect size = 0.2) (Figure 3).

Additional t-test statistical analyses of nodal degree and BC were performed for each hub between controls and patients and reported in Supplementary Table 1. We observed a significant decrease of nodal degree in the hubs lost in nfvPPA and a trend of increase of betweenness centrality in the new hubs. Significances survived after multiple comparisons correction (FDR) and after controlling for local gray matter volume (gray matter volume of the cube for each node was added as a covariate).

Unlike the SPN, the DMN hubs were distributed in a similar architecture for patients and controls: they were located bilaterally in the frontal pole, precuneus, posterior cingulate and paracingulate, lateral occipital lobe, and the right angular gyrus. No significant differences were found in local metrics (Supplementary Figure 3).

3.3.2 Post-hoc analysis: Recalculation of hubs in healthy controls.—To test whether there was an underlying topological difference unique to nfvPPA, we simulated the damaged SPN of patients in controls. To this end, we subtracted the damaged hubs in the patients' SPN from the SPN of the healthy controls and recalculated the distribution of hubs. We assumed that hubs lost by nfvPPA patients would create similar disruption when subtracted from the healthy SPN network. We found that the recalculated location of hubs in the control group resembled those found in the diseased brain, with hubs located in the more anterior left IFG and the right pars opercularis of IFG, right MFG and the right SPL (Supplementary Figure 4).

3.3.3 Post-hoc analysis: Correlation analysis in the right hemisphere with Rule Violation errors.—As a post-hoc analysis, we sought to better understand the impact of the right hemisphere nodes that became hubs in the altered network of nfvPPA. We analyzed Rule Violation (RV) errors from the Delis-Kaplan Executive Function System (Delis et al., 2001). Rule Violation errors represent responses that violated the explicit rules of each paradigm and they have been previously shown to be associated with frontal regions in the right hemisphere (Possin et al., 2009). These errors included failure to shift errors in Trail Making Number-Letter Switching, set-loss errors in Letter Fluency (FAS) or set-loss

errors in Design Fluency Filled, Empty, and Switching conditions. The average number of errors across the subtests available was used to define the number of RV errors for each subject. This RV scale was available in 18 patients out of 20. We performed correlation analyses between the nodal metrics in the hubs of the right hemisphere and the functional connectivity (FC) within the SPN's hubs and the Rule Violation errors in the patients' executive function testing. We found a significant negative correlation ($r = -0.47$, $p<0.05$) between the average number of RV errors and the FC of the newly recruited hub in the right opIFG with the left opIFG (Figure 4). Although the results were not corrected for multiple comparisons, this was the only significant correlation found among all hubs. No significant correlation was found with volume loss, or nodal metrics within these nodes. We then created a composite speech production (SP) score, including the weighted average of the WAB Spontaneous Speech rating and severity scores for Apraxia of Speech and Dysarthria from the Motor Speech Evaluation (Wertz et al. 1984) as described in Mandelli et al., 2014. We correlated the SP score with the FC of the left IFG (epicenter) that was lost in nfvPPA with the other SPN hubs. We found a significant positive correlation within the left hemisphere ($r = 0.6$, $P<0.001$) (Figure 4). No significance was found in the right hemisphere.

3.3.4 Global measures of the networks.—Within the chosen range of thresholds, the patients' SPN network density was significantly decreased compared to controls. In fact, all the normalized global measures were altered in the nfvPPA SPN compared to controls (Supplementary Table 2). Global efficiency and assortativity were significantly decreased, characteristic path length, cluster coefficient, and modularity increased, although the latter didn't survive after multiple comparisons correction across the entire range of thresholds. Due to the significantly different density metrics in patients compared to controls, we investigated whether there was a two-way interaction between group and density by using an analysis of variance (R packages, https://cran.r-project.org/). This interaction was not significant between group and density, which indicates that the group effect on the connectivity metrics is not influenced by differences in network density between the two cohorts. Supplementary Table 2 lists the statistical significance of the main effects for each of the thresholds and connectivity metrics.

Most global metrics of the DMN did not show any significant differences between controls and patients, whether for density or normalized metrics (Supplementary Table 3). One exception was the characteristic path length, which showed a trend toward significance that did not survive correction for multiple comparisons.

Network density and selected normalized global metrics are displayed in Figure 5, with different thresholds for each network in the two cohorts.

4. Discussion

This study provides new evidence for altered organization within the speech production network in nfvPPA using graph theoretical analysis. Hubs were lost in left-hemisphere regions most affected by the disease, and additional hubs were recruited more anteriorly within the left frontal regions and in the right hemisphere. Behaviorally, speech production

and rule violation errors correlated with functional connectivity strength in the left and right hemisphere respectively. Global network metrics characterized the SPN as more segregated and less efficiently wired in nfvPPA than in the healthy brain. These changes were specific to the SPN and did not occur in the DMN used as reference network.

Distribution of hubs and nodal metrics within the speech production network

In this study, we showed that the nfvPPA group presented a different configuration of hubs in the SPN compared to controls. The SPN of nfvPPA patients lost some critical nodes in the left parietal regions and in the SMC but also presented alternative hubs that were located more anteriorly to the IFG pars opercularis, in the MFG and in the right side of the brain (Figure 2). These differences were specific to the SPN and did not occur in the DMN. We also simulated the hub damage in healthy subjects. We found that the set of nodes that were designated as hubs had a similar configuration between controls and patients (Supplementary Figure 3).

Together, these graph theory analyses highlight the importance of understanding the specific drivers of hub loss and gain, in addition to measuring structural or functional changes in the context of neurodegenerative disease. In this study, the hub alterations were best explained by decreases in nodal degree for the lost hubs, and increases in betweenness centrality for the gained hubs (Figure 3). This change in hub configuration was not consistent with decreases in gray matter volume in the site where hubs were lost or gained. In other words, the graph theoretical alterations in the network were better accounted for by functional rather than structural changes.

Indeed, the loss of functional connectivity in left frontal regions was associated with impairments in speech production, while higher functional connectivity to right frontal regions was associated with better behavioral monitoring (fewer Rule Violation errors) (Figure 4). These behaviors were not correlated with volume changes in the corresponding hubs. This is consistent with previous literature suggesting that damage to hubs causes particularly severe functional impairment due to their critical role in integrative brain processing (Buckner et al., 2009; Brier et al., 2014; Mattson et al., 2016). For example, in Alzheimer’s disease, the aggregation of Aβ seems to be driven by the level of neuronal activity of the cortical hubs, suggesting that the connectivity properties of neuronal subpopulations may play a role in determining their intrinsic sensitivity to stress (Mattson et al., 2016).

The pathogenesis underlying neurodegenerative disease is accompanied by a series of pathophysiological events such as axonal degeneration, synapse loss, dendritic retraction (Sweeney, et al., 2018; Yates, 2012) and the propagation of misfolded proteins (Raj et al., 2012; Yates, 2012). These events impact structural and functional properties to different extents in different regions. Indeed, focal atrophy can be accompanied by hypo- or hyper-connectivity within and across networks, depending on the organization of global and local connections (Dickerson & Sperling, 2009, Pasquini et al., 2015, García-Cordero et al., 2015). Pathogenesis might disrupt network integrity in many ways, such as reducing network efficiency, altering the balance between damaged and spared networks and/or activating compensatory mechanisms (Pievani, et al., 2014; Tahmasian et al., 2016).

Our findings suggest that focal atrophy in nfvPPA has an impact at the network level by altering the functional connectivity within the regions.

In a recent study from our group, we showed that damage in nfvPPA originated from a vulnerable region of the brain, called the *epicenter*. In nfvPPA, the epicenter is the pars opercularis of the IFG. The damage then spreads in a predictable pattern to functionally and structurally connected regions, according to the strength of connectivity in the healthy brain network (Mandelli et al., 2016). The findings in the current study are consistent with this previous data: regions most connected to the disease epicenter experienced the greatest loss of connections in the diseased brain and, therefore, lost their critical role in information processing and their status as hubs. Specifically, the disease epicenter of the IFG pars opercularis is functionally and structurally connected to the SMC through the aslant tract and to the SMG through the superior longitudinal fasciculus, and disease spreads through these pathways (Whitwell et al., 2010; Galantucci et al., 2011; Grossman, 2012; Grossman et al., 2013; Mahoney et al., 2013; Schwindt et al., 2013; Mandelli et al., 2014). These regions (SMC and SMG) consistently experienced the greatest hub loss in this study. When epicenter regions and their connections are targeted by disease, other functionally connected regions that are less compromised within the same network may become critical sites, at least relatively. Overall, these findings suggest that in nfvPPA, the damaged network tends towards a more modular organization.

Increased functional segregation in the speech production network

In the SPN of nfvPPA, we found a significant increase of cluster coefficient and a trend towards increased modularity, after normalization with random networks. Cluster coefficient computes how strongly inter-connected neighboring nodes are to one another, thus reflecting the local efficiency with which information is transferred within a network (Bullmore & Sporns 2009). Modularity implies a set of nodes whose connections with each other are much stronger than their connections to nodes in different modules, thus quantifying the degree to which a network may be subdivided into different modules. Our results suggest that within this network, communities of nodes experienced an abnormal increase in local connectivity, with an inclination to segregate into sparsely organized, smaller communities. However, in this study, an increase in modularity did not achieve statistical significance, and we speculate that this could be related to the focality of this disease at an early stage. In the healthy brain, network modularity could allow regions to specialize in specific functions but may also be protective in the neurodegenerative brain by preventing early propagation of perturbation through the system and inhibiting cascading failure (Buldyrev et al., 2010; Fornito et al., 2015). Indeed, this appears to be the case for nfvPPA. We showed that in the early stages of the disease damage was initially relatively specific to the SPN network. This same disease process spared the DMN.

Decreased functional integration and resilience in the speech production network

In the nfvPPA-affected SPN, we found a significant increase in the characteristic path length and a consequent decrease in global efficiency. We also found a decrease in assortativity. These results suggest that the flow of information was compromised and that global integration across distant regions and modules became less efficient. Because some

pathways in the network were disrupted, the neuronal signal needed to rely on longer routes, with a consequent efficiency cost. Moreover, the decrease of assortativity suggests that in the degenerating SPN, nodes of high degree tend to connect with nodes of low degree, instead of linking with nodes of similar degree. This could be interpreted as an attempt to recruit lower-degree nodes when higher-degree nodes start to be affected by the disease.

Limitations of the study

The application of graph theory to describe neurobiological processes is a new field with limited methodological consensus, in particular on optimal network construction and graph theoretical parameters (Zalesky et al. 2010, Fornito et al., 2010; Wig et al., 2011; Smith et al., 2011; Craddock et al., 2012; Van Essen et al., 2012; Garrison et al., 2015). Additionally, our analysis was limited to only two networks known to be involved in specific neurodegenerative diseases, and they were studied independently. Further studies, especially longitudinal ones, are needed to model the spatial and temporal dimension of the functional networks. Very few studies have attempted to approach this phenomenon (Hutchison et al., 2013; Hansen et al., 2015).

Conclusion

We used graph theory analysis of resting-state fMRI data to demonstrate altered topology in the SPN in nfvPPA. The nfvPPA network became more segregated and less efficient, globally and locally. These changes were network-specific and did not occur in the DMN, supporting the hypothesis of selective network vulnerability. Graph theoretical analyses are particularly valuable in studying neurodegenerative diseases because functional and structural connections may react differently to pathogenesis at a network level. Global and local metrics can also provide specific characterizations of disease progression (Bullmore & Sporns 2009; Fornito et al., 2015) and may offer viable biomarkers for future behavioral and pharmaceutical interventions.

Supplementary Material

Refer to Web version on PubMed Central for supplementary material.

Acknowledgements:

The study was supported by grants from the National Institutes of Health (NINDS R01NS050915, NIDCD K24DC015544, NIA U01AG052943, NIA P50AG023501, NIA P01AG019724, R01AG038791, U01AG045390, U54NS092089 Alzheimer's Disease Research Center of California (03–75271 DHS/ADP/ARCC); Larry L. Hillblom Foundation; John Douglas French Alzheimer's Foundation; Koret Family Foundation; Consortium for Frontotemporal Dementia Research; and McBean Family Foundation.

References

Agosta F, Sala S, Valsasina P, Meani A, Canu E, Magnani G, Cappa SF, Scola E, Quatto P, Horsfield MA, Falini A, Comi G, Filippi M (2013). Brain network connectivity assessed using graph theory in frontotemporal dementia. Neurology, 81(2), 134–43. [PubMed: 23719145]

Agosta F, Galantucci S, Valsasina P, Canu E, Meani A, Marcone A, Magnani G, Falini A, Comi G, Filippi M (2014). Disrupted brain connectome in semantic variant of primary progressive aphasia. Neurobiol Aging, 35(11), 2646–55. [PubMed: 24970567]

Biswal B, Yetkin FZ, Haughton VM, Hyde JS (1995). Functional connectivity in the motor cortex of resting human brain using echo-planar MRI. Magn Reson Med, 34 (4), 537–541. [PubMed: 8524021]

Blondel VD, Guillaume JL, Hendrickx JM, de Kerchove C, Lambiotte R (2008). Local leaders in random networks. Phys Rev E Stat Nonlin Soft Matter Phys, 77(3 Pt 2), 036114. [PubMed: 18517468]

Boccaletti S, Latora V, Moreno Y, Chavez M, Hwang DU (2006). Complex networks: structure and dynamics. Physics Reports 424, 175–30.

Bonakdarpour B, Rogalski EJ, Wang A, Sridhar J, Mesulam MM, and Hurley RS (2017) Functional connectivity is reduced in early stage primary progressive aphasia when atrophy is not prominent. Alzheimer Dis Assoc Disord. 31(2): 101–106. [PubMed: 28288010]

Buckner RL, Sepulcre J, Talukdar T, Krienen FM, Liu H, Hedden T, Andrews-Hanna JR, Sperling RA, Johnson KA (2009). Cortical hubs revealed by intrinsic functional connectivity: mapping, assessment of stability, and relation to Alzheimer's disease. J Neurosci, 29 (6), 1860–1873. [PubMed: 19211893]

Brier MR, Thomas JB, Fagan AM, Hassenstab J, Holtzman DM, Benzinger TL, Morris JC, Ances BM (2014). Functional connectivity and graph theory in preclinical Alzheimer's disease. Neurobiol Aging, 35(4), 757–68. [PubMed: 24216223]

Buldyrev SV, Parshani R, Paul G, Stanley HE, Havlin S (2010). Catastrophic cascade of failures in interdependent networks. Nature, 464, 1025–1028. [PubMed: 20393559]

Bullmore E, Sporns O (2009). Complex brain networks: graph theoretical analysis of structural and functional systems. Nat Rev Neurosci, 10 (3), 186–198. [PubMed: 19190637]

Catani M, Mesulam MM, Jakobsen E, Malik F, Martersteck A, Wieneke C, Thompson CK, Thiebaut de Schotten M, Dell'Acqua F, Weintraub S, Rogalski E (2013). A novel frontal pathway underlies verbal fluency in primary progressive aphasia. Brain, 136, 2619–28. [PubMed: 23820597]

Collins JA, Montal V, Hochberg D, Quimby M, Mandelli ML, Makris N, Seeley WW, Gorno-Tempini ML, Dickerson BC (2017). Focal temporal pole atrophy and network degeneration in semantic variant primary progressive aphasia. Brain, 140, 457–471. [PubMed: 28040670]

Craddock RC, James GA, Holtzheimer PE, Hu XP, and Mayberg HS (2012). A whole brain fMRI atlas generated via spatially constrained spectral clustering. Hum. Brain Mapp, 33, 1914–1928. [PubMed: 21769991]

Damoiseaux J, Rombouts S, Barkhof F, Scheltens P, Stam C, Smith S, & Beckmann C (2006). Consistent resting-state networks across healthy subjects. Proceedings of the National Academy of Sciences, 103 (37), 13848–13853.

de Calignon A, Polydoro M, Suarez-Calvet M, William C, Adamowicz DH, Kopeikina KJ, Pitstick R, Sahara N, Ashe KH, Carlson GA, Spires-Jones TL, Hyman BT (2012). Propagation of tau pathology in a model of early Alzheimer's disease. Neuron, 73, 685–97. [PubMed: 22365544]

de Haan W, Pijnenburg YA, Strijers RL, van der Made Y, van der Flier WM, Scheltens P, Stam CJ (2009). Functional neural network analysis in frontotemporal dementia and Alzheimer's disease using EEG and graph theory. BMC Neurosci, 10,101. [PubMed: 19698093]

Delis D, Kaplan EB, Kramer J (2001). The Delis-Kaplan Executive Function System. The Psychological Corporation.

Dickerson BC, Sperling RA (2009). Large-scale functional brain network abnormalities in Alzheimer's disease: insights from functional neuroimaging. Behav Neurol, 21, 63–75. [PubMed: 19847046]

Folstein MF, Folstein SE, McHugh PR (1975). Mini-mental state: A practical method for grading the cognitive state of patients for the clinician. J Psychiatr Res, 12(3), 189–98. [PubMed: 1202204]

Fornito A, Zalesky A, Bullmore ET (2010). Network scaling effects in graph analytic studies of human resting-state fMRI data. Front Syst Neurosci, 4:22. [PubMed: 20592949]

Fornito A, Zalesky A, Breakspear M (2015). The connectomics of brain disorders. Nat Rev Neurosci, 6(3), 159–72.

Kramer JH, Jurik J, Sha SJ, Rankin KP, Rosen HJ, Johnson JK, Miller BL (2003). Distinctive neuropsychological patterns in frontotemporal dementia, semantic dementia, and Alzheimer disease. Cogn Behav Neurol, 16, 211–18. [PubMed: 14665820]

Kruschwitz JD, List D, Waller L, Rubinov M, Walter H (2015). GraphVar: A user-friendly toolbox for comprehensive graph analyses of functional brain connectivity, Journal of Neuroscience Methods, 245, 107–15. [PubMed: 25725332]

Freeman LC (1977). A set of measures of centrality based on betweenness. Sociometry, 40, 35–41.

Frost B, Diamond MI (2010). Prion-like mechanisms in neurodegenerative diseases. Nat Rev Neurosci, 11, 155–9. [PubMed: 20029438]

Galantucci S, Tartaglia MC, Wilson SM, Henry ML, Filippi M, Agosta F, Dronkers NF, Henry RG, Ogar JM, Miller BL, Gorno-Tempini ML (2011) White matter damage in primary progressive aphasias: a diffusion tensor tractography study. Brain 134 (Pt 10): 3011–29. [PubMed: 21666264]

Garrison KA, Scheinost D, Finn ES, Shen X, Constable RT (2015). The (in)stability of functional brain network measures across thresholds. Neuroimage, 118, 651–61. [PubMed: 26021218]

García-Cordero I, Sedeño L, Fraiman D, Craiem D, de la Fuente LA, Salamone P, Serrano C, Sposato L, Manes F, Ibañez A (2015). Stroke and Neurodegeneration Induce Different Connectivity Aberrations in the Insula. Stroke, 46(9), 2673–2677. [PubMed: 26185182]

Gorno-Tempini ML, Dronkers NF, Rankin KP, Ogar JM, Phengrasamy L, Rosen HJ, Johnson JK, Weiner MW, Miller BL (2004). Cognition and anatomy in three variants of primary progressive aphasia. Ann Neurol, 55, 335–346. [PubMed: 14991811]

Gorno-Tempini ML, Ogar JM, Brambati SM, Wang P, Jeong JH, Rankin KP, Dronkers NF, Miller BL (2006). Anatomical correlates of early mutism in progressive nonfluent aphasia. Neurology, 67(10), 1849–51. [PubMed: 16931509]

Gorno-Tempini ML, Hillis AE, Weintraub S, Kertesz A, Mendez M, Cappa SF, Ogar JM, Rohrer JD, Black S, Boeve BF, Manes F, Dronkers NF, Vandenberghe R, Rascovsky K, Patterson K, Miller BL, Knopman DS, Hodges JR, Mesulam MM, Grossman M (2011). Classification of primary progressive aphasia and its variants. Neurology, 76, 1006–14. [PubMed: 21325651]

Greicius MD, Krasnow B, Reiss AL, Menon V (2003). Functional connectivity in the resting brain: a network analysis of the default mode hypothesis. Proc Natl Acad Sci USA, 100 (1), 253–258. [PubMed: 12506194]

Greicius MD, Srivastava G, Reiss AL, Menon V (2004) Default-mode network activity distinguishes Alzheimer's disease from healthy aging: evidence from functional MRI. Proc Natl Acad Sci USA, 101, 4637–42. [PubMed: 15070770]

Grossman M, Mickanin J, Onishi K, Hughes E, D'Esposito M, Ding XS, Alavi A, Reivich M (1996). Progressive nonfluent aphasia: language, cognitive, and PET measures contrasted with probable Alzheimer's disease. J Cogn Neurosci, 8, 135–154. [PubMed: 23971420]

Grossman M (2012). The non-fluent/agrammatic variant of primary progressive aphasia. Lancet Neurol, 11, 545–555. [PubMed: 22608668]

Grossman M, Powers J, Ash S, McMillan C, Burkholder L, Irwin D, Trojanowski JQ (2013). Disruption of large-scale neural networks in nonfluent/agrammatic variant primary progressive aphasia associated with frontotemporal degeneration pathology. Brain Lang, 127, 106–120. [PubMed: 23218686]

Guo CC, Kurth F, Zhou J, Mayer EA, Eickhoff SB, Kramer JH, Seeley WW (2012). One-year test–retest reliability of intrinsic connectivity network fMRI in older adults. NeuroImage, 61(4), 1471–1483. [PubMed: 22446491]

Hansen EC, Battaglia D, Spiegler A, Deco G, Jirsa VK (2015). Functional connectivity dynamics: modeling the switching behavior of the resting state. Neuroimage, 105, 525–35. [PubMed: 25462790]

Horwitz B & Rowe JB (2011). Functional Biomarkers for Neurodegenerative Disorders Based on the Network Paradigm. Prog. Neurobiology, 95(4), 505–509.

Howard D & Patterson KE (1992). The Pyramids and Palm Trees Test: A test of semantic access from words and pictures. Thames Valley Test Company.

Hutchison RM, Womelsdorf T, Gati JS, Everling S, Menon RS (2013). Resting-state networks show dynamic functional connectivity in awake humans and anesthetized macaques. Hum Brain Mapp, 34(9), 2154–77. [PubMed: 22438275]

Kertesz A (1980). Western aphasia battery. London, Ontario, University of Western Ontario.

Latora V, Marchiori M (2001). Efficient behavior of small-world networks. Phys Rev Lett, 87(19).

Liu L, Drouet V, Wu JW, Witter MP, Small SA, Clelland C, Duff K (2012). Trans-Synaptic spread of tau pathology in vivo. PLoS One 7(2).

Mahoney CJ, Malone IB, Ridgway GR, Buckley AH, Downey LE, Golden HL, Ryan NS, Ourselin S, Schott JM, Rossor MN, Fox NC, Warren JD (2013). White matter tract signatures of the progressive aphasias. Neurobiol Aging, 34, 1687–1699. [PubMed: 23312804]

Mandelli ML, Caverzasi E, Binney RJ, Henry ML, Lobach I, Block N, Amirbekian B, Dronkers N, Miller BL, Henry RG, Gorno-Tempini ML (2014). Frontal white matter tracts sustaining speech production in primary progressive aphasia. J Neurosci, 34(29), 9754–67. [PubMed: 25031413]

Mandelli ML, Vilaplana E, Brown JA, Hubbard HI, Binney RJ, Attygalle S, Santos-Santos MA, Miller ZA, Pakvasa M, Henry ML, Rosen HJ, Henry RG, Rabinovici GD, Miller BL, Seeley WW, Gorno-Tempini ML (2016). Healthy brain connectivity predicts atrophy progression in non-fluent variant of primary progressive aphasia. Brain, 139(10), 2778–2791. [PubMed: 27497488]

Mattson N, Schott JM, Hardy J, Turner MR, Zetterberg H (2016). Selective vulnerability in neurodegeneration: insights from clinical variants of Alzheimer's disease. J Neurol Neurosurg Psychiatry, 87(9), 1000–4. [PubMed: 26746185]

Mesulam MM (1982). Slowly progressive aphasia without generalized dementia. Ann Neurol, 11, 592–598. [PubMed: 7114808]

Meunier D, Achard S, Morcom A, Bullmore E (2009). Age-changes in modular organization of human brain functional networks. Neuroimage, 44(3), 715–23. [PubMed: 19027073]

Minati L, Varotto G, D'Incerti L, Panzica F, Chan D (2013). From brain topography to brain topology: relevance of graph theory to functional neuroscience. Neuroreport, 24(10), 536–543. [PubMed: 23660679]

Nestor PJ, Graham NL, Fryer TD, Williams GB, Patterson K, Hodges JR (2003). Progressive non-fluent aphasia is associated with hypometabolism centred on the left anterior insula. Brain, 126(11), 2406–2418. [PubMed: 12902311]

Newman ME (2002). Assortative mixing in networks. Physical review letters, 89(20), 208701. [PubMed: 12443515]

Newman ME (2003). Mixing patterns in networks. Physical Review E, 67(2), 026126.

Newman ME (2006). Modularity and community structure in networks. Proc Natl Acad Sci USA, 103, 8577–82. [PubMed: 16723398]

Pasquini L, Scherr M, Tahmasian M, Meng C, Myers NE, Ortner M, Mühlau M, Kurz A, Förstl H, Zimmer C, Grimmer T, Wohlschläger AM, Riedl V, Sorg C (2015). Link between hippocampus' raised local and eased global intrinsic connectivity in AD. Alzheimers Dement, 11(5), 475–484. [PubMed: 25043909]

Pievani M, Filippini N, Van Den Heuvel MP, Cappa SF, & Frisoni GB (2014). Brain connectivity in neurodegenerative diseases from phenotype to proteinopathy. Nature Reviews Neurology, 10(11), 620–633. [PubMed: 25287597]

Possin KL, Brambati S,M, Rosen HJ, Johnson JK, Pa J, Weiner MW, Miller BL, Kramer JH (2009). Rule violation errors are associated with right lateral prefrontal cortex atrophy in neurodegenerative disease. J Int Neuropsychol Soc.15(3):354–64. [PubMed: 19402921]

Raj A, Kuceyeski A, & Weiner M (2012). A network diffusion model of disease progression in dementia. Neuron, 73(6), 1204–1215. [PubMed: 22445347]

Rajapakse JC, Giedd JN, Rapoport JL (1997). Statistical approach to segmentation of single-channel cerebral MR images. IEEE Trans Med Imaging, 16(2), 176–186. [PubMed: 9101327]

Rosen HJ, Gorno-Tempini ML, Goldman WP, Perry RJ, Schuff N, Weiner M, Feiwell R, Kramer JH, Miller BL (2002). Patterns of brain atrophy in frontotemporal dementia and semantic dementia. Neurology, 58, 198–208. [PubMed: 11805245]

Rubinov M, Sporns O (2010). Complex network measures of brain connectivity: uses and interpretations. Neuroimage, 52, 1059–1069. [PubMed: 19819337]

Salvador R, Suckling J, Coleman MR, Pickard JD, Menon D, Bullmore E (2005). Neurophysiological architecture of functional magnetic resonance images of human brain. Cereb. Cortex, 15(9), 1332–1342. [PubMed: 15635061]

Sanz-Arigita EJ, Schoonheim MM, Damoiseaux JS, Rombouts SA, Maris E, Barkhof F, Scheltens P, Stam CJ (2010). Loss of 'small-world' networks in Alzheimer's disease: graph analysis of fMRI resting-state functional connectivity. PLoS One 5(11).

Satterthwaite TD, Elliott MA, Gerraty RT, Ruparel K, Loughead J, Calkins ME, Eickhoff SB, Hakonarson H, Gur RC, Gur RE, Wolf DH (2013). An improved framework for confound regression and filtering for control of motion artifact in the preprocessing of resting-state functional connectivity data. Neuroimage, 2013, 64: 240–56.

Schwindt GC, Graham NL, Rochon E, Tang-Wai DF, Lobaugh NJ, Chow TW, Black SE (2013). Whole-brain white matter disruption in semantic and Nonfluent variants of primary progressive aphasia. Hum Brain Mapp, 3, 973–984.

Sedeño L, Couto B, García-Cordero I, Melloni M, Baez S, Morales Sepúlveda JP, Fraiman D, Huepe D, Hurtado E, Matallana D, Kuljis R, Torralva T, Chialvo D, Sigman M, Piguet O, Manes F, Ibanez A (2016). Brain network organization and social executive performance in frontotemporal dementia. J Int Neuropsychol Soc, 22, 250–262. [PubMed: 26888621]

Sedeño L, Piguet O, Abrevaya S, Desmaras H, García-Cordero I, Baez S, Alethia de la Fuente L, Reyes P, Tu S, Moguilner S, Lori N, Landin-Romero R, Matallana D, Slachevsky A, Torralva T, Chialvo D, Kumfor F, García AM, Manes F, Hodges JR, Ibanez A (2017). Tackling variability: A multicenter study to provide a gold-standard network approach for frontotemporal dementia. Hum Brain Mapp, 38(8), 3804–3822. [PubMed: 28474365]

Sweeney MD, Sagare AP, & Zlokovic BV (2018). Blood-brain barrier breakdown in Alzheimer disease and other neurodegenerative disorders. Nature Reviews Neurology. 14(3):133–15 [PubMed: 29377008]

Smith S, Miller K, Salimi-Khorshidi G, Webster M, Beckmann C, Nichols T, Ramsey J, Woolrich M (2011). Network modelling methods for FMRI. NeuroImage, 54, 875–891. [PubMed: 20817103]

Sporns O, Chialvo DR, Kaiser M, Hilgetag CC (2004). Organization, development and function of complex brain networks. Trends Cogn Sci, 8(9), 418–425. [PubMed: 15350243]

Sporns O, Honey CJ, Kötter R (2007). Identification and classification of hubs in brain networks. PLoS One, 2(10).

Stam CJ, Reijneveld JC (2007). Graph theoretical analysis of complex networks in the brain. Nonlinear Biomed Phys, 1(1), 3. [PubMed: 17908336]

Strogatz SH (2001). Exploring complex networks. Nature, 410, 268–277. [PubMed: 11258382]

Supekar K, Menon V, Rubin D, Musen M, and Greicius MD (2008). Network analysis of intrinsic functional brain connectivity in Alzheimer's disease. PLoS Comput. Biol, 4(6).

Tahmasian M, Shao J, Meng C, Grimmer T, Diehl-Schmid J, Yousefi BH, Förster S, Riedl V, Drzezga A, Sorg C (2016). Based on the network degeneration hypothesis: separating individual patients with different neurodegenerative syndromes in a preliminary hybrid PET/MR study. Journal of Nuclear Medicine, 57(3), 410–415. [PubMed: 26585059]

Taubert M, Lohmann G, Margulies DS, Villringer A, & Ragert P (2011). Long-term effects of motor training on resting-state networks and underlying brain structure. Neuroimage, 57(4), 1492–1498. [PubMed: 21672633]

Tian L, Wang J, Yan C, He Y (2011). Hemisphere- and gender related differences in small-world brain networks: a resting state functional MRI study. Neuroimage, 54, 191–202. [PubMed: 20688177]

Tijms BM, Möller C, Vrenken H, Wink AM, de Haan W, van der Flier WM, Stam CJ, Scheltens P, Barkhof F (2013). Single-subject grey matter graphs in Alzheimer's disease. PLoS One, 8(3).

van den Heuvel MP, Hulshoff Pol HE (2010). Exploring the brain network: a review on resting-state fMRI functional connectivity. Eur Neuropsychopharmacol, 20(8), 519–34. [PubMed: 20471808]

van den Heuvel MP, de Lange SC, Zalesky A, Seguin C, Yeo BTT, Schmidt R (2017). Proportional thresholding in resting-state fMRI functional connectivity networks and consequences for patient-control connectome studies: Issues and recommendations. NeuroImage, 152, 437–449. [PubMed: 28167349]

Van Essen DC, Ugurbil K, Auerbach E, Barch D, Behrens TE, Bucholz R, Chang A, Chen L, Corbetta M, Curtiss SW, Della Penna S, Feinberg D, Glasser MF, Harel N, Heath AC, Larson-Prior L, Marcus D, Michalareas G, Moeller S, Oostenveld R, Petersen SE, Prior F, Schlaggar BL, Smith

SM, Snyder AZ, Xu J, Yacoub E, WU-Minn HCP Consortium. (2012). The Human Connectome Project: a data acquisition perspective. Neuroimage, 62, 2222–31. [PubMed: 22366334]

van Wijk BC, Stam CJ, Daffertshofer A (2010). Comparing brain networks of different size and connectivity density using graph theory. PLoS One, 5(10).

Watts DJ and Strogatz SH (1998). Collective dynamics of 'small-world' networks". Nature, 393(6684), 440–442. [PubMed: 9623998]

Watts DJ (2004). The 'new' science of networks. Annu Rev Sociol, 30, 243–270.

Wertz RT, LaPointe LL, & Rosenbek JC (1984). Apraxia of speech in adults: The disorder and its management. New York, Grune and Stratton.

Whitwell JL, Avula R, Senjem ML, Kantarci K, Weigand SD, Samikoglu A, Edmonson HA, Vemuri P, Knopman DS, Boeve BF, Petersen RC, Josephs KA, Jack CR, Jr. (2010). Gray and white matter water diffusion in the syndromic variants of frontotemporal dementia. Neurology, 74, 1279–1287. [PubMed: 20404309]

Wig GS, Schlaggar BL, Petersen SE (2011). Concepts and principles in the analysis of brain networks. Ann NY Acad Sci, 1224, 126–146. [PubMed: 21486299]

Wilson SM, Dronkers NF, Ogar JM, Jang J, Growdon ME, Agosta F, Henry ML, Miller BL, Gorno-Tempini ML (2010). Neural correlates of syntactic processing in the nonfluent variant of primary progressive aphasia. J Neurosci, 30(50), 16845–54. [PubMed: 21159955]

Wilson SM, Galantucci S, Tartaglia MC, Rising K, Patterson DK, Henry ML, Gorno-Tempini ML (2011). Syntactic processing depends on dorsal language tracts. Neuron, 72, 397–403. [PubMed: 22017996]

Xia M, Wang J, He Y (2013) BrainNet viewer: a network visualization tool for human brain connectomics. PLoS ONE, 8(7).

Yates D (2012). Neurodegenerative disease: Neurodegenerative networking. Nature Reviews Neuroscience, 13(5), 288.

Zalesky A, Fornito A, Harding IH, Cocchi L, Yücel M, Pantelis C, Bullmore ET (2010). Whole-brain anatomical networks: does the choice of nodes matter? Neuroimage, 50, 970–983. [PubMed: 20035887]

Zhao X, Liu Y, Wang X, Liu B, Xi Q, Guo Q, Jiang H, Jiang T, Wang P (2012). Disrupted small-world brain networks in moderate Alzheimer's disease: a resting-state fMRI study. PLoS One, 7(3).

Zhou J, Gennatas ED, Kramer JH, Miller BL, Seeley WW (2012). Predicting regional neurodegeneration from the healthy brain functional connectome. Neuron, 73, 1216–1227. [PubMed: 22445348]

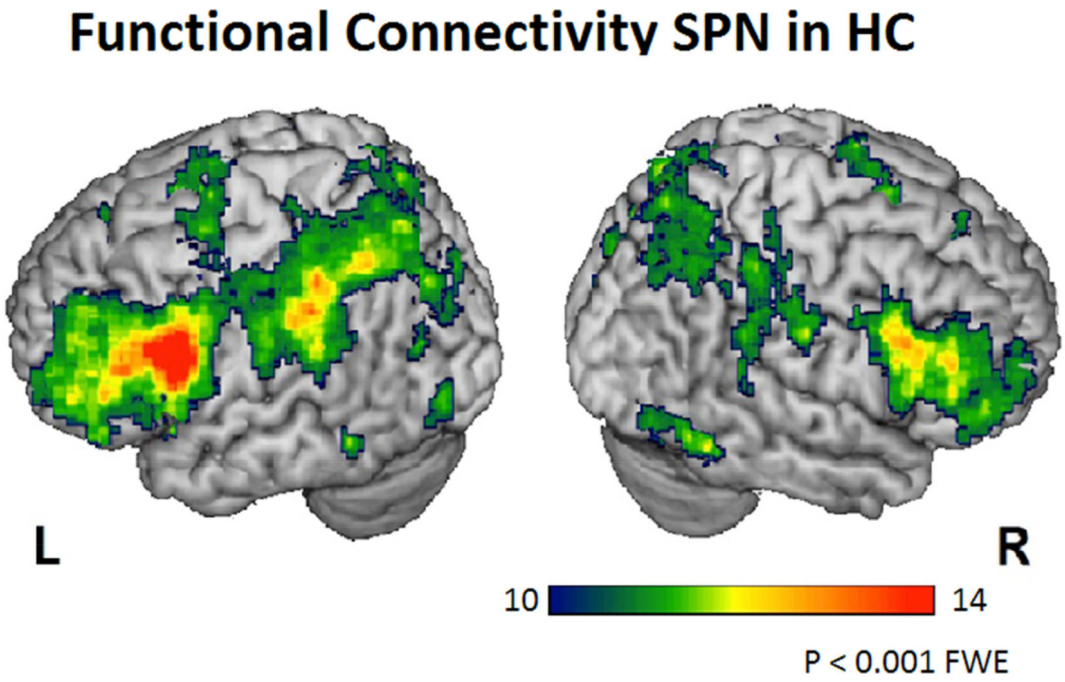

Figure 1:
Statistical parametric maps of functional connectivity of the SPN in a group of healthy controls with seed-ROI in the left pars opercularis of IFG (P<0.001 FWE)

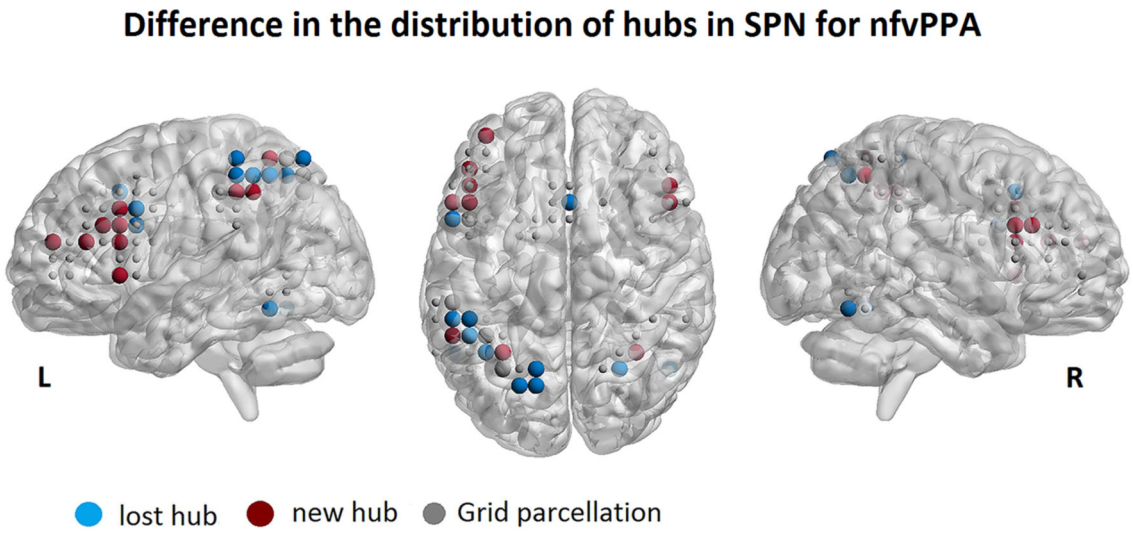

Figure 2:
Difference in the distribution of hubs in the SPN for the group of nfvPPA patients. The lost hubs (light blue) and new hubs (dark red) are displayed respect the distribution of the healthy control group.

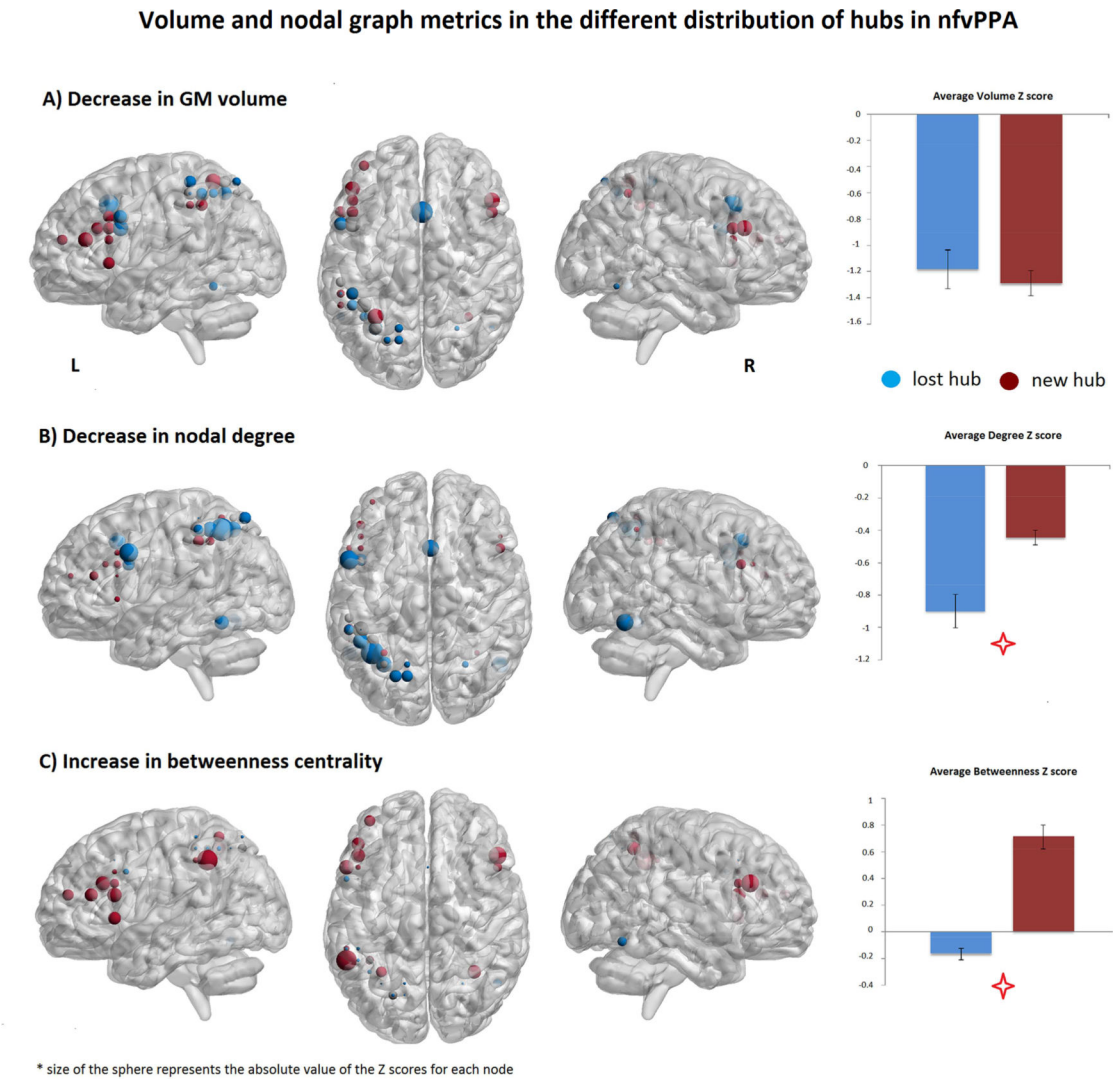

Figure 3:

The Z scores of the structural (GM volume) and nodal metrics (nodal degree and betweenness centrality) of the lost and new hubs in nfvPPA were calculated and displayed. The size of the sphere is proportional to: A) gray matter volume loss (bigger spheres = greater volume loss; B) decrease in nodal degree (bigger spheres = greater loss in number of connections); C) increase in betweenness (bigger spheres = higher value of betweenness centrality). As the figure suggests, the blue spheres (lost hubs in nfvPPA) have greater loss of degree while the red ones (new hubs in nfvPPA) have an increase of betweenness centrality. These differences were statistically significant between the group of lost and new hubs in patients. On the contrary there were not differences in volume between lost and gained hubs in nfvPPA.

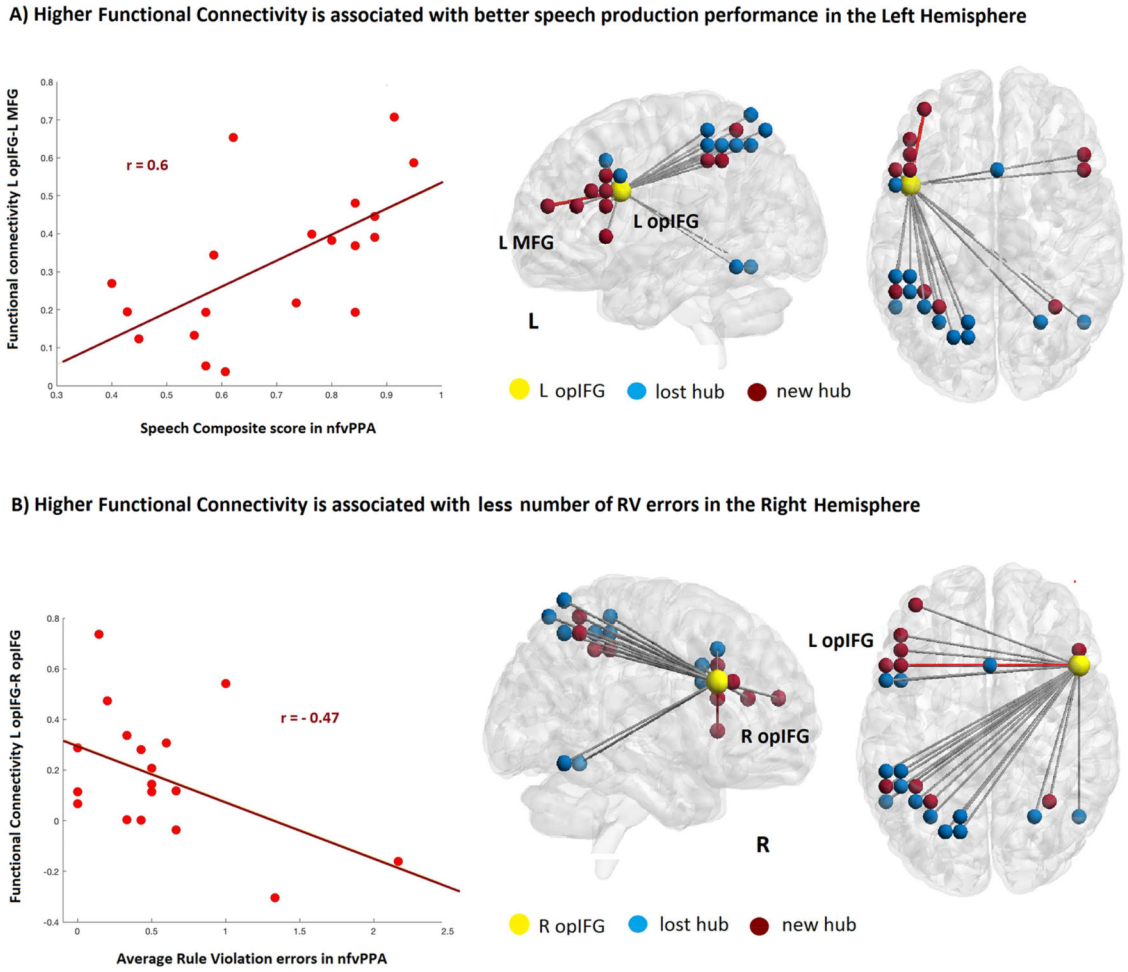

Figure 4:

Pair-wise correlations between hubs functional connectivity (FC) and cognitive measures in nfvPPA. A) The correlation between the FC with the left IFG and all the lost and new hubs in nfvPPA showed a significant positive association with the composite speech production (SP) score that indicates higher FC associated with better speech production performance. B) The correlation between the FC with the right IFG and all the lost and new hubs in nfvPPA showed a significant negative association with the number of RV errors that indicates higher FC associated with fewer numbers of errors.

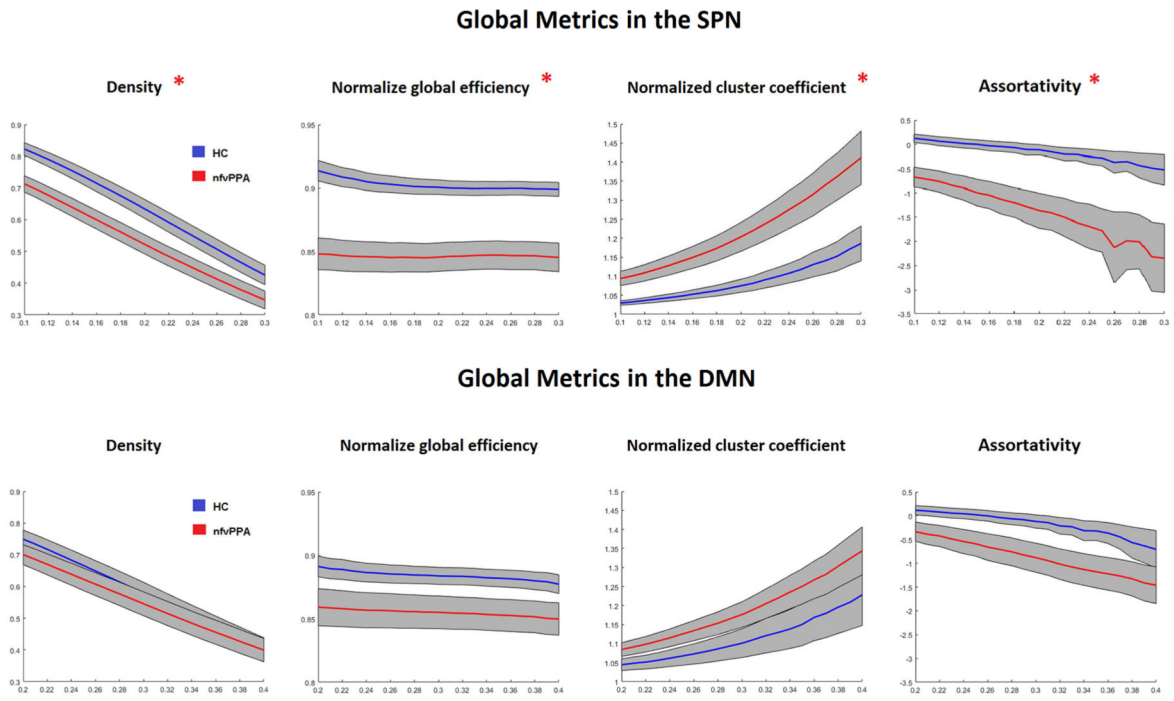

Figure 5:

Error bar plots of normalized global network parameters for the healthy controls (blue) and nfvPPA patients (red) for both speech production and default mode networks across the range of chosen thresholds. The red star indicated significant different between the two groups over the entire range of thresholds.

Table 1.

Demographic and cognitive evaluation

	NfvPPA (n=20)	Cognitive Controls (n=20)
Age	68.8 (7.3)	68.6 (6.0)
Gender (F/M)	9/11	9/11
Handedness (R/Other)	17/3	15/4^
Education	18.2 (3.6)	16.9 (2.4)
Disease duration	3.57 (1.43)	N/A
MMSE (30)	26.2 (3.7) *	29.1 (1.5)
CDR Total	0.55 (0.2)	N/A
Visuospatial function		
Benson copy (17)	14.7 (1.7) *	15.9 (1.2)
Memory		
Benson delay (17)	10.2 (2.9) *	12.9 (2.0)
CVLT-SF 10 min (9)	4.55 (2.8) *	7.3 (1.9)
CVLT-SF recognition	7.5 (2.6)	8.5 (0.8)
Executive function		
Digit span backwards	3.6 (1.4) *	5.4 (1.5)
Modified Trails (lines /sec)	0.25 (0.2) *	0.6 (0.2)
Language		
Boston Naming Test (15)	10.5 (2.9) *	14.5 (0.8)
Phonemic Fluency	5.7 (3.0) *	15.2 (4.7)
Semantic Fluency	9.8 (4.8) *	23.0 (4.6)
Speech Fluency (WAB, 10)	6.9 (2.1) *	10 (0)
Repetition (WAB, 100)	84.6 (15.6) *	100 (0)
Word recognition (WAB, 60)	59.3 (1.7)	60 (0)
Sequential Commands (WAB, 80)	71.9 (9.2) *	80 (0)
AOS (MSE, 7 max)	2.5 (1.5) *	0 (0)
Dysarthria (MSE, 7)	1.7 (1.9) *	0 (0)
Syntax Comprehension (100)	94.6(5.8) *	100(0)
PPTP (52)	47.4 (6.3)	51 (0.8)

* p <.05 patients vs controls.

^ Handedness was unknown for one participant.

MMSE = mini-mental state examination, CDR = clinical dementia rating, CVLT-MS = California Verbal Learning Test – Short Form, WAB = Western Aphasia Battery, MSE = Motor Speech Evaluation; AOS = apraxia of speech, PPTP = pyramids and palm trees test pictures. ^ 3 missing